Isolation and Characterizations of Quinone Analogue-Resistant Mutants of *bo*-Type Ubiquinol Oxidase from *Escherichia coli*†

Mariko Sato-Watanabe,‡ Tatsushi Mogi,*,‡ Kimitoshi Sakamoto,§ Hideto Miyoshi,§ and Yasuhiro Anraku‡,||

Department of Biological Sciences, Graduate School of Science, University of Tokyo, Hongo, Bunkyo-ku, Tokyo 113-0033, and Division of Applied Life Sciences, Graduate School of Agriculture, Kyoto University, Kitashirakawa, Sakyo-ku, Kyoto 606-8502, Japan

Received May 19, 1998

ABSTRACT: Cytochrome *bo* is a member of the heme-copper terminal oxidase superfamily and serves as a four-subunit ubiquinol oxidase in the aerobic respiratory chain of *Escherichia coli*. To probe the location and structural properties of the ubiquinol oxidation site, we isolated and characterized five or 10 spontaneous mutants resistant to either 2,6-dimethyl-1,4-benzoquinone, 2,6-dichloro-4-nitrophenol, or 2,6-dichloro-4-dicyanovinylphenol, the potent competitive inhibitors for the oxidation of ubiquinol-1 [Sato-Watanabe, M., Mogi, T., Miyoshi, H., Iwamura, H., Matsushita, K., Adachi, O., and Anraku, Y. (1994) *J. Biol. Chem*. *269*, 28899−28907]. Analyses of the growth yields and the ubiquinol-1 oxidase activities of the mutant membranes showed that the mutations increased the degree of the resistance to the selecting compounds. Notably, several mutants showed the cross-resistance. These data indicate that the binding sites for substrate and the competitive inhibitors are partially overlapped in the ubiquinol oxidation site. All the mutations were linked to the expression vector, and 23 mutations examined were all present in the C-terminal hydrophilic domain (Pro^{96}-His^{315}) of subunit II. Sequencing analysis revealed that seven mutations examined are localized near both ends of the cupredoxin fold. Met248Ile, Ser258Asn, Phe281Ser, and His284Pro are present in a quinol oxidase-specific (Qox) domain and proximal to low-spin heme *b* in subunit I and the lost Cu_A site in subunit II, whereas Ile129Thr, Asn198Thr, and Gln233His are rather scattered in a three-dimensional structure and closer to transmembrane helices of subunit II. Our data suggest that the Qox domain and the Cu_A end of the cupredoxin fold provide the quinol oxidation site and are involved in electron transfer to the metal centers in subunit I.

Cytochrome *bo* is a four-subunit ubiquinol oxidase in the aerobic respiratory chain of *Escherichia coli* (see refs *1*−*4* for recent reviews) and belongs to a superfamily of the heme-copper terminal oxidases (*5*−*7*). The enzyme catalyzes the four-electron reduction of dioxygen with two molecules of ubiquinol-8 (Q_8H_2)[1] and can establish a proton electrochemical gradient across the cytoplasmic membrane not only via scalar protolytic reactions but also via a proton pump mechanism (*8*). Cytochrome *bd*, an alternative two-subunit ubiquinol oxidase in the aerobic respiratory chain, is structurally unrelated to cytochrome *bo* (*1*, *2*) and does not pump protons (*8*).

Subunit I binds all the redox metal centers, low-spin heme *b*, high-spin heme *o*, and Cu_B, and serves as a reaction field for redox-coupled proton pumping (*1*−*4*). Heme *o* and Cu_B form the heme-copper binuclear center where dioxygen reduction takes place (*1*−*4*). Functional assembly of the redox metal centers requires the coexpression of subunits III and IV (*9*−*11*), although they are dispensable for the catalytic activity (*12*). Subunit II does not contain any redox metal center (*1*−*4*); however, photoaffinity cross-linking studies with an azido-ubiquinone indicated the presence of a quinol oxidation site in subunit II (*13*). The oxidation of quinols by cytochrome *bo* proceeds in cooperation of two quinol/quinone binding sites; a low-affinity quinol oxidation site (Q_L) is in dynamic equilibrium with the membrane quinone pool (*14*), whereas a high-affinity quinone binding site (Q_H) is close to both the Q_L site and low-spin heme *b* and mediates intramolecular electron transfer (*15*−*20*). The Q_H site tightly binds both Q_8 and Q_8H_2 (*15*) and can stabilize a ubisemiquinone radical during turnover (*20*−*22*). Sato-Watanabe et al. (*15*, *18*−*20*) postulated that the Q_H site serves as a transient electron reservoir for two-electron supply from the Q_L site and gates electron flux allowing sequential one-

† This work was supported in part by Grants-in-aid for Scientific Research on Priority Areas (08249106 and 09257213 to T.M.) and for Scientific Research (B) (08458202 to T.M.) and (C) (08660136 to H.M.) from the Ministry of Education, Science, Sports and Culture, Japan. This is paper XXXV in the series Structure−function studies on the *E. coli* cytochrome *bo*.

* To whom correspondence should be addressed. Fax 81-3-3814-2583. E-mail mogi@biol.s.u-tokyo.ac.jp.

‡ University of Tokyo.

§ Kyoto University.

|| Present address: Department of Biosciences, Teikyo University of Science and Technology, Uenohara, Kitatsuru, Yamanashi 409-0193, Japan.

[1] Abbreviations: MBQ, methyl-1,4-benzoquinone; DMBQ, 2-6-dimethyl-1,4-benzoquinone; 2-EtO-Q_2, 2-ethoxy-3-methoxy-5-methyl-6-geranyl-1,4-benzoquinone; 3-EtO-Q_2, 3-ethoxy-2-methoxy-5-methyl-6-geranyl-1,4-benzoquinone; HHQNO, 2-heptyl hydroxyquinoline-*N*-oxide; NOR, nitric oxide reductase; PC15, 2,6-dichloro-4-nitrophenol; PC16, 2,6-dichloro-4-dicyanovinylphenol; PC24, 2-chloro-4,6-dinitrophenol; PC31, 2,6-dichloro-4-cyanophenol; Q_n, ubiquinone-*n*; Q_nH_2, ubiquinol-*n*; Q_H, a high-affinity quinone binding site; Q_L, a low-affinity quinol oxidation site; Qox domain, quinol oxidase-specific domain.

S0006-2960(98)01184-2 CCC: $15.00
Published on Web 08/26/1998

electron transfer from the Q_L site to heme *b*.

Cytochrome *c* oxidase is another member of the heme-copper terminal oxidases (*5*−*7*). The binuclear purple copper center (Cu_A) present in the C-terminal hydrophilic domain of subunit II serves as an electron input site and mediates one-electron transfer from ferrocytochrome *c* to low-spin heme *a* in subunit I (*23*−*27*; see ref *28* for a review). The ligands of Cu_A have been determined by site-directed mutagenesis studies (*23*−*25*) and crystallographic studies (*29*−*32*) and are located at one end of the cupredoxin fold (Greek key β-barrel structure), which is proximal to heme *a* (*29*−*32*). Cytochrome *c* oxidases and quinol oxidases share subunits I, II, and III and carry out a similar mechanism for dioxygen reduction and redox-coupled proton pumping, despite differences in electron donors, substrate oxidation sites in subunit II, bound heme species in subunit I, and subunit structures (*5*, *6*). Structural similarities of the oxidases and the organization of the oxidase operons (*7*, *33*−*37*) strongly indicate that eubacterial quinol oxidases have evolved from cytochrome *c* oxidase of Gram-positive bacteria (*7*), which has been further derived from the redox enzymes for anaerobic nitrate respiration (*38*−*40*). Subunit II of quinol oxidases retains two transmembrane helices and the cupredoxin fold in the C-terminal hydrophilic domain but lacks almost all ligands of Cu_A (*33*−*37*). Therefore, quinol oxidases may have acquired the Q_L site by minor modifications of subunit II or addition of a unique structural domain to the C-terminus of subunit II.

Here, we report for the first time the isolation and characterization of the *E. coli* cytochrome *bo* mutants that were resistant to three potent Q_L site inhibitors, either 2,6-dimethyl-1,4-benzoquinone (DMBQ) or substituted phenols. Growth phenotypes and enzymatic properties of the ubiquinone analogue-resistant mutants indicated that the mutations were related to the Q_L site. Locations and properties of the mutations suggest that the quinol oxidase-specific (Qox) domain and/or the Cu_A end of the cupredoxin fold in the C-terminal hydrophilic domain of subunit II provide the Q_L site, which is proximal to heme *b* in subunit I.

MATERIALS AND METHODS

Bacterial Strains and Plasmids. ST2592/pMFO4 (Δ*cyo*-Cm^r Δ*cyd*-Km^r/cyo^+ Ap^r; ref *41*) can express the plasmid borne cytochrome *bo* as a sole terminal oxidase and was used for isolation of the quinone analogue-resistant mutants. A single copy expression vector pMFO4 carries the wild-type cytochrome *bo* operon and contains a gene-engineered *Nhe*I site in the 3′ portion of the *cyoA* gene (*41*). pHN3795-1 (cyo^+ Ap^r), a derivative of pBR322, carries the 10 kb *Bam*HI−*Pvu*II fragment containing the *cyo* operon (*42*). pBR4-O9B and pHNFO11P-O9B (*10*) are derivatives of pHN3795-1 and pMFO4, respectively, and carry the *cyo* operon where eight gene-engineered unique restriction sites have been introduced within (*41*, *43*) and outside (*10*) the coding sequences.

Preparation of Crude Membranes. *E. coli* cells were aerobically grown in a rich medium (*44*) containing 15 μg/mL sodium ampicillin and harvested at the late exponential phase of growth ($Abs_{650} = 0.6$). The cells were washed and treated with lysozyme-EDTA, and the resultant sphaeroplasts were disrupted by two passages through a French Press. The unbroken cells and sphaeroplasts were removed by centrifugation at 12000*g* for 5 min. Crude membranes were recovered by centrifugation at 180000*g* for 1.5 h, and suspended in 10 mM Tris-HCl (pH 7.4) containing 3 mM sodium EDTA and 10% sucrose.

Quinol Oxidase Assay. Quinol oxidase activity was determined spectroscopically at 25 °C as described previously (*14*, *45*). The reaction mixture contains 50 mM Tris-HCl (pH 7.4), 0.1% sucrose monolaurate SM-1200 (Mitsubishi-Kasei Food Co., Tokyo), and 3 μg/mL membrane proteins. The reaction was started by the addition of ubiquinols, and the activity was calculated with a molar extinction coefficient of 12 250 at 275 nm for an oxidized form of ubiquinones (*46*). Effects of ubiquinone analogues were examined after preincubation of the enzyme with the analogues at 25 °C for 1 min. Double reciprocal plot analysis was carried out at final concentrations of Q_1H_2 from 25 to 150 μM or the Q_2H_2 analogues from 5 to 100 μM.

Determination of Growth Yield of Intact Cells. Strain ST2592/pMFO4 or /pHN3795-1 was grown aerobically at 37 °C for 2 days in 5 mL of minimal medium A (*47*) supplemented with 15 μg/mL sodium ampicillin, 0.5% sodium succinate, and the ubiquinone analogues at final concentrations of 5 to 700 μM. Alternatively, cells were grown anaerobically in a sealed jar (*41*). The absorbance at 650 nm of the culture medium was determined with a Shimadzu UV-160 spectrophotometer before and after centrifugation at 5000*g* and at 4 °C for 10 min. The growth yield was defined as the net absorbance change.

Screening of Spontaneous Mutants Resistant to Quinone Analogues. ST2592/pMFO4 cells were grown aerobically at 37 °C for 3−5 days in 5 mL of minimal medium A supplemented with 0.5% sodium succinate, 15 μg/mL ampicillin and inhibitors, either 200 μM PC15, 100 μM PC16, or 20 μM DMBQ. After single colony isolation on LB-glucose-ampicillin plates, plasmids were recovered from the mutant candidates and used for retransformation of ST2592. The transformants were grown anaerobically on LB-glucose-ampicillin plates and then grown aerobically in the above-mentioned liquid medium for 15 h to confirm that the mutations were linked to plasmid DNAs.

Identification of Point Mutations Conferring Resistance to Ubiquinone Analogues. The 1.1 kb *Nar*I−*Nhe*I [−299 to +801; the nucleotide number from the transcription start site (*48*)] and the 2.5 kb *Nhe*I−*Eco*RI (802−3347) fragments were isolated from the mutant pMFO4 and replaced with the counterparts of the wild-type pMFO4. Alternatively, the 4.5 kb *Kpn*I−*Kpn*I (328−4803) fragment of the mutant plasmids was substituted by the corresponding fragment of pBR4-O9B to give pBR4-KK. The 0.80-kb *Bam*HI−*Nhe*I (20−801) fragment of pBR4-KK containing the 0.47 kb *Kpn*I−*Nhe*I fragment of the mutant plasmids was subcloned at the corresponding sites of pHNFO11P-O9B. The 0.32 kb *Nhe*I−*Sal*I (802−1167) fragment of pBR4-KK was replaced with the counterpart of the wild-type pBR4-O9B to give pBR4-NH. Subsequently, the derivatives of pMFO4, pHNFO11P-O9B and pBR4-O9B were used for complementation tests. Finally, nucleotide sequences of the 0.47 kb *Kpn*I−*Nhe*I or the 0.32 kb *Nhe*I−*Sal*I fragment carrying the mutations were determined by plasmid direct sequencing with a model 373A DNA sequencer or a Prism 310 Genetic

Analyzer (Applied Biosystems Inc.) using custom-made primers.

Miscellaneous. Determinations of protein concentration and heme content were as described previously (*41*, *44*). PC15 (2,6-dichloro-4-nitrophenol), PC16 (2,6-dichloro-4-dicyanovinylphenol), and PC31 (2,6-dichloro-4-cyanophenol) (*14*, *49*, *50*), 2-EtO-Q_2 (2-ethoxy-3-methoxy-5-methyl-6-geranyl-1,4-benzoquinone), and 3-EtO-Q_2 (2-methoxy-3-ethoxy-5-methyl-6-geranyl-1,4-benzoquinone) (*45*) were synthesized as described previously. MBQ (methyl-1,4-benzoquinone) and DMBQ were obtained from Tokyo Kasei Co., and HHQNO (2-heptyl-4-hydroxyquinoline *N*-oxide) was purchased from Sigma. Q_1 and Piericidin A were generous gifts from Eisai Co. Ltd. (Tsukuba) and N. Takahashi (University of Tokyo), respectively. Other chemicals were commercial products of analytical grade.

RESULTS

Screening of Q_L Site Inhibitors for Isolation of Quinone Analogue-Resistant Mutants. To identify the potent Q_L site inhibitors that can be used for isolation of the ubiquinone analogue-resistant mutants, the effect of piericidin A, HHQNO (*51*, *52*), benzoquinones (MBQ and DMBQ), and substituted phenols (PC15, PC16, and PC31) (*14*) on respiration of the ST2592/pMFO4 cells with succinate was examined. MBQ and DMBQ at 10 μM or PC15 and PC16 at 100 μM reduced the succinate oxidase activity of the carbon-starved cells to 2−4% of the control value whereas the effects of piericidin A, HHQNO and PC31 at 100 μM were insignificant (91−97% residual activities). Thus, MBQ, DMBQ, PC15, and PC16 are permeable to the *E. coli* membranes and can inhibit cytochrome *bo* in the intact cells. Subsequently, succinate:Q_1 reductase activity of the cytoplasmic membrane vesicles was determined in the presence of the ubiquinone analogues. MBQ, DMBQ, and PC16 had a small effect on succinate dehydrogenase (86−100% residual activities), but PC15 competed the ubiquinone reduction site and reduced succinate:Q_1 reductase activity to 6% of the control level. Accordingly, PC15 can simultaneously inhibit succinate dehydrogenase and cytochrome *bo* in succinate respiration of the intact cells.

Effect of Quinone Analogues on Aerobic Growth of E. coli Cells. To determine the concentration of the quinone analogues that is sufficient for the suppression of the aerobic growth, we examined their effect on the growth yield of ST2592/pMFO4, which can express the plasmid-borne cytochrome *bo* as a sole terminal oxidase. The growth yields in the presence of the quinone analogues were evaluated as a net absorbance change of the culture medium at 650 nm after 12 h growth in the minimal-0.5% succinate medium. We found that DMBQ, PC15, and PC16 completely suppressed the aerobic growth of the cells at final concentrations of 20, 200, and 100 μM, respectively (Figure 1), but did not affect at all the anaerobic growth (data not shown). Due to the degradation in the culture medium, MBQ had no effect on the growth yield. The I_{50} values, defined as the inhibitor concentrations required for 50% reduction of the growth yield, were determined to be about 6, 70, and 60 μM for DMBQ, PC15, and PC16, respectively (Figure 1), which are at least 1 order of magnitude greater than their K_i values for the Q_1H_2 oxidation (*14*). In ST2592/pHN3795-1, the I_{50} values for the ubiquinone analogues were elevated to about 50, 220, and 400 μM, respectively, due to the gene dosage effect (Figure 1). These results provide further support for their primary inhibition site at the terminal oxidase.

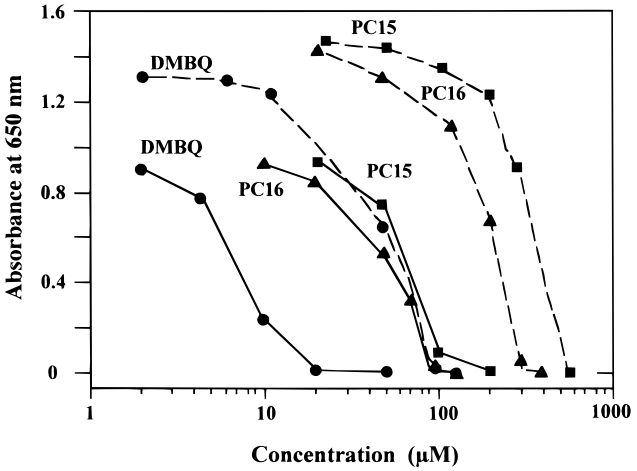

FIGURE 1: Effects of ubiquinone analogues on the growth yield of a terminal oxidase-deficient mutant ST2592 harboring a single copy vector pMFO4 (solid line) or a multicopy vector pHN3795-1 (broken line). Cells were aerobically grown in minimal medium A supplemented with 0.5% succinate and 15 or 100 μg/mL sodium ampicillin in the presence of quinone analogues at concentrations as indicated.

Isolation and Growth Properties of Quinone Analogue-Resistant Mutants. From the aerobic culture of ST2592/pMFO4 in the presence of either 20 μM DMBQ, 200 μM PC15, or 100 μM PC16, we isolated independently five or 10 spontaneous mutants resistant to each quinone analogue (Table 1). Retransformation of ST2592 with recovered plasmids confirmed that all the mutations were linked to plasmid DNAs. All the mutants grew normally in the minimal-succinate medium in the absence of the ubiquinone analogues as did the wild-type (i.e., 87−97% of the wild-type control), except the mutants PC16−S2 and DMBQ−S2 that reduced their growth yields to 52 and 66%, respectively. The substituted phenol-resistant mutants except PC15−S3, −S10, PC16−S8 to −S10 were sensitive to DMBQ, and all the DMBQ-resistant mutants except DMBQ−S2 were sensitive to both PC15 and PC16 (Table 1). The I_{50} values of PC15−S3 and −S8 for PC15 increased from 70 μM of the wild-type value to 200 and 220 μM, respectively, whereas that of DMBQ−S1 showed only a slight change (90 μM) (Figure 2). The I_{50} values of PC15−S3, PC15−S8, and DMBQ−S1 for DMBQ shifted from 6 μM of the wild-type control to 29, 14, and 21 μM, respectively (Figure 2). Unexpectedly, PC15−S3, −S10, PC16−S8 to −S10 and DMBQ−S2 showed cross-resistance (Table 1).

Enzymatic Properties of Mutant Membranes. The expression levels and the enzymatic properties of the mutant oxidases were examined using crude membranes. Western blotting analysis with the anti-cytochrome *bo* antiserum showed the expression levels of subunits I and II were comparable to those of the wild-type membranes (data not shown), suggesting that the analogue-resistant mutations did not affect the stability of the enzyme.

Effects of the mutations on the Q_1H_2 oxidase activity were kinetically examined in details (Table 1). Because of our

Table 1: Effects of Q_L Site Inhibitors on the Aerobic Growth of Quinone Analogue-Resistant Mutants and on the Q_1H_2 Oxidase Activity of the Mutant Membranes

	growth yield (%)				K_i (μM)[a]			
mutant	none	PC15	PC16	DMBQ	PC15	PC16	DMBQ	K_m (μM)[a], Q_1H_2
wild-type	100 (0.994)[b]	<1	1	1	3.4	3.0	0.31	36
PC15−S1	100 (0.938)	82	94	1	62	26	0.30	32
PC15−S2	100 (0.932)	78	71	1	47	35	0.21	27
PC15−S3	100 (0.932)	47	75	84	18	13	1.2	29
PC15−S4	100 (0.936)	57	18	1	18	20	0.28	37
PC15−S5	100 (0.948)	39	27	1	105	87	0.31	36
PC15−S6	100 (0.945)	61	23	3	17	18	13	33
PC15−S7	100 (0.937)	91	16	1	21	21	0.54	40
PC15−S8	100 (0.925)	58	22	1	19	25	13	51
PC15−S9	100 (0.953)	66	98	2	24	24	0.30	43
PC15−S10	100 (0.934)	78	92	31	24	25	6.2	45
PC16−S1	100 (0.905)	80	85	1	23	44	0.46	33
PC16−S2	100 (0.513)	84	90	2	24	18	0.21	32
PC16−S3	100 (0.915)	72	69	1	17	31	0.72	56
PC16−S4	100 (0.962)	31	37	1	28	29	0.14	43
PC16−S5	100 (0.914)	65	43	1	19	42	0.31	28
PC16−S6	100 (0.915)	84	90	1	15	23	0.24	43
PC16−S7	100 (0.897)	22	48	1	14	16	0.26	26
PC16−S8	100 (0.951)	68	31	94	32	36	9.7	21
PC16−S9	100 (0.915)	8	14	88	14	18	1.2	32
PC16−S10	100 (0.861)	58	100	95	115	108	21	27
DMBQ−S1	100 (0.896)	2	4	53	3.7	3.7	3.3	25
DMBQ−S2	100 (0.648)	3	100	90	20	19	1.7	33
DMBQ−S3	100 (0.954)	1	2	90	4.2	3.8	2.4	28
DMBQ−S4	100 (0.964)	2	4	50	1.2	0.8	4.3	22
DMBQ−S5	100 (0.942)	1	1	45	3.9	3.6	3.7	43

[a] Q_1H_2 oxidase activity of the crude membranes was determined in the presence of 100 μM PC15, 100 μM PC16 or 10 μM DMBQ at the protein concentration of 3 μg/mL. Kinetic parameters were determined by double-reciprocal plots at the Q_1H_2 concentrations of 25−150 μM. [b] The mutants were aerobically grown overnight in the presence of either 200 μM PC15, 100 μM PC16, or 20 μM DMBQ. The growth yields were determined as a net absorbance change of the culture medium at 650 nm and are expressed as a percentage of the control value in the absence of the quinone analogues.

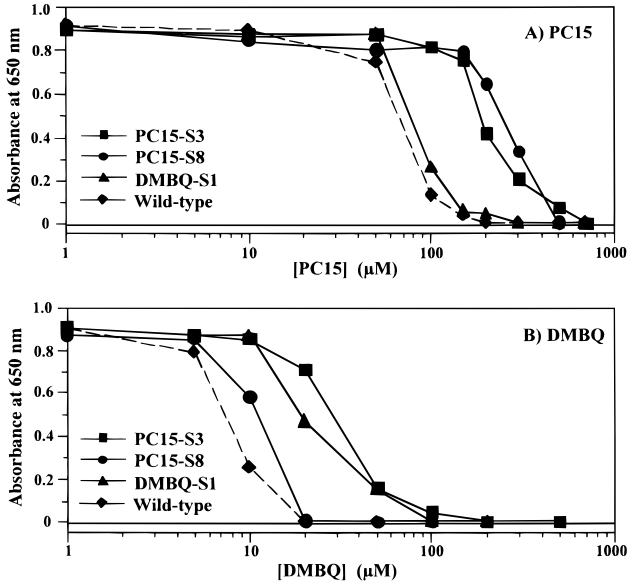

FIGURE 2: Effects of PC15 and DMBQ on the growth yield of the PC15-resistant and DMBQ-resistant mutants. Cells of ST2592/pMFO4−PC15−S3, −PC15−S8 or -DMBQ-S1 were grown aerobically as described in the legend to Figure 1.

strategy for the screening of the ubiquinone analogue-resistant mutants, we found only slight variations in the K_m values for Q_1H_2 (36 μM of the wild-type vs 21−56 μM of the mutants). Modes of the inhibition by DMBQ, PC15, and PC16 in the mutant membranes were all competitive against Q_1H_2 as reported for the wild-type enzyme (*14*). In the substituted phenol-resistant mutants, the K_i values for PC15 and PC16 increased 4−34-fold and 4−36-fold, respectively, in comparison of those for 3.4 and 3.0 μM, respectively, of the wild-type control. These results suggest that the binding site recognizes the overlapping structure of these two substituted phenols, and are consistent with our previous proposal that the substituent at the 4-position protrudes from the phenol ring-binding site (*14*). In contrast, the K_i value for DMBQ remained almost unchanged except PC15−S3, −S6, −S8, −S10, PC16−S3, and −S8 to −S10. The K_i values in these mutants increased 2.3−68-fold from 0.31 μM of the wild-type control, and that of PC15−S10 was even larger than those of the DMBQ-resistant mutants (6.2 vs 1.7−4.3 μM). It should be noted that the cross-resistance of the Q_1H_2 oxidase activities in PC15−S6, −S8, and PC16−S3 was inconsistent with the growth phenotypes (Table 1).

In the DMBQ-resistant mutants, the K_i values for DMBQ were 5.5−19-fold larger than the wild-type control and those for substituted phenols varied from 0.8 to 20 μM (Table 1). DMBQ−S4, which has the largest K_i value among the DMBQ-resistant mutants, showed weak hypersensitivity to the substituted phenols, and DMBQ−S2 exhibited the cross-resistance as expected from the growth yield.

Next, we examined the kinetic properties of the mutant enzymes for the oxidation of Q_2H_2 analogues with a bulky ethoxy group at either the 2- or the 3-position of the ubiquinone ring (Table 2). As we have previously shown for the wild-type enzyme (*45*), the replacement of the 2-methoxy group with an ethoxy group decreased the affinity for substrate 3−6-fold and the V_{max} values to about one-

Table 2: Kinetic Properties of the Quinone Analogue-Resistant Mutant Enzymes in the Oxidation of the Q_2H_2 Analogues

	K_m (μM)		
mutant	Q_2H_2	3-EtO-Q_2H_2	2-EtO-Q_2H_2
wild-type	15 (100)[a]	16 (100)	56 (23)
PC15−S1	22 (100)	21 (95)	66 (18)
PC15−S2	13 (100)	17 (92)	55 (14)
PC15−S3	26 (100)	25 (100)	81 (23)
PC15−S4	13 (100)	14 (93)	80 (26)
PC15−S5	14 (100)	14 (100)	74 (18)
PC15−S7	11 (100)	14 (100)	61 (22)
PC15−S8	23 (100)	22 (76)	80 (17)
PC15−S10	16 (100)	14 (83)	67 (19)
PC16−S6	14 (100)	16 (87)	72 (18)
PC16−S8	21 (100)	23 (100)	71 (21)
PC16−S10	15 (100)	17 (93)	77 (29)
DMBQ−S1	21 (100)	16 (68)	92 (20)
DMBQ−S2	22 (100)	17 (73)	89 (22)
DMBQ−S3	26 (100)	26 (85)	118 (19)
DMBQ−S4	27 (100)	27 (93)	103 (18)
DMBQ−S5	25 (100)	27 (91)	80 (14)

[a] Relative V_{max} values (percentage of the Q_2H_2 oxidase activities) are indicated in the parentheses.

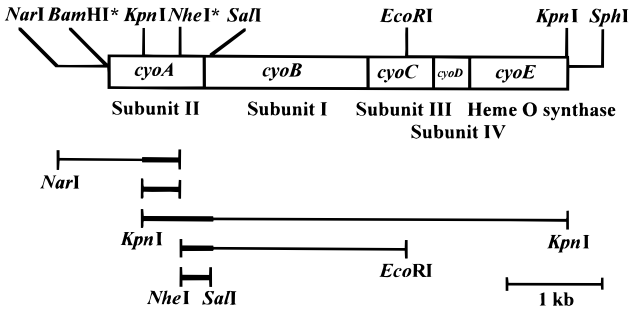

FIGURE 3: Physical map of the cytochrome *bo* operon (*cyoABCDE*) and restriction fragments used for subcloning of the quinone analogue-resistant mutations. The gene-engineered *Bam*HI (*10*) and *Nhe*I (*41*) sites are indicated by asterisks. The mutations for PC15−S3, −S7, −S8, −S10, PC16−S1, −S5, and −S6 were complemented by the 1.1 kb *Nar*I−*Nhe*I, the 0.47 kb *Kpn*I−*Nhe*I, and the 4.5 kb *Kpn*I−*Kpn*I fragments, and those for PC15−S1, −S2, −S5, −S6, −S9, PC16−S2, −S3, −S5, −S8 to −S10, DMBQ-S1 to −S5 by the 4.5 kb *Kpn*I−*Kpn*I, the 2.5 kb *Nhe*I−*Eco*RI, and the 0.32 kb *Nhe*I−*Sal*I fragments. Segments carrying the mutations are indicated by thick bars.

fifth of the Q_2H_2 and 3-EtO-Q_2H_2 oxidase activities, suggesting that the mutations examined did not affect the recognition of the ubiquinone ring. These data indicate that the binding sites for substrates (i.e., Q_1H_2 and Q_8H_2) and two kinds of the competitive inhibitors (DMBQ and substituted phenols) are partially overlapped in the Q_L site.

Identification of Point Mutations. To localize the ubiquinone analogue-resistant mutations, we constructed a series of recombinant plasmids and carried out genetic complementation tests (Figure 3). The derivatives of pMFO4, pHNF11P-O9B, or pBR-O9B were introduced into a terminal oxidase-deficient mutant ST2592, and then transformants were cultured aerobically in the presence of the quinone analogues used for the first selection. Complementation tests revealed that the 1.1 kb *Nar*I−*Nhe*I, the 0.47 kb *Kpn*I−*Nhe*I, and the 4.5 kb *Kpn*I−*Kpn*I fragments from PC15−S3, −S7, −S8, −S10, PC16−S1, −S5, and −S6 contained the mutations. Thus, these mutations are present in the overlapping 0.47 kb *Kpn*I−*Nhe*I fragment corresponding to Pro^{96}-Lys^{253} of subunit II. Analysis with the 4.5 kb *Kpn*I−*Kpn*I, the 2.5 kb *Nhe*I−*Eco*RI, and the 0.32 kb *Nhe*I−*Sal*I fragments revealed that the 0.32 kb *Nhe*I−*Sal*I fragment corresponding to Leu^{254}-His^{315} of subunit II and Met^{1}-Ser^{51} of subunit I contained the mutations for PC15−S1, −S2, −S5, −S6 and −S9, PC16−S2, −S3, −S5, −S8 to −S10, and DMBQ−S1 to −S5. Since His^{13}-His^{54} of subunit I including helix 0 (Glu^{14}-Thr^{36}; ref *41*) was not required for the Q_1H_2 oxidase activity[2] and the N-terminus of subunit I can be fused to the C-terminus of subunit II without loss of the activity (53), all the mutations must be linked to the C-terminal hydrophilic domain (Pro^{96}-His^{315}) of subunit II.

Subsequently, sequencing analysis determined the PC15−S3, −S5, −S10, PC16−S1, −S6, DMBQ−S3, and −S5 mutations as Ile129Thr, Ser258Asn, Asn198Thr, Met248Ile, Gln233His, His284Gln, and Phe281Ser, respectively (Figure 4). In a three-dimensional model for the two-subunit cytochrome *bo* (Figure 5), the mutations are localized near both ends of the cupredoxin fold in the C-terminal hydrophilic domain of subunit II. Ile129Thr, Asn198Thr, and Gln233His are rather scattered and closer to transmembrane helices of subunit II, whereas Met248Ile, Ser258Asn, Phe281Ser, and His284Pro are proximal to the lost Cu_A binding site in subunit II (*25*) and to heme *b* in subunit I (Figure 5). It should be noted that subunit II of terminal quinol oxidases contains a unique structural domain (Qox domain) with the 60 amino acid residue long at the C-terminus (Figure 4). In cytochrome *bo*, the α_2-β_{11}-α_3 structure has been identified in the Qox domain (*31*). The localization of Met248Ile, Ser258Asn, Phe281Ser and His284Pro within or near the Qox domain and their proximity to both the lost Cu_A site and heme *b* suggest the functional importance of the Qox domain in the oxidation of substrates. However, the Qox domain is not well conserved in quinol oxidases (Figure 4), and the ubiquinone analogue-resistant mutations did not affect the K_m values for substrates (Tables 1 and 2). Therefore, the Qox domain and/or the Cu_A end of the cupredoxin fold appear to provide the Q_L site at the periplasmic surface of the membrane.

DISCUSSION

Recent crystallographic studies on bacterial (*29*, *32*) and mammalian (*30*, *54*) cytochrome *c* oxidases confirmed the axial ligands of the metal centers determined by site-directed mutagenesis studies on subunits I (*1*−*4*) and II (*23*, *28*, *55*, *56*). The atomic structures of cytochrome *c* oxidases provided us with new insights into molecular mechanism of redox-coupled proton pumping, dioxygen reduction, and electron transfer from cytochrome *c* to heme *a* through Cu_A. The structural similarity of the *E. coli* cytochrome *bo* with cytochrome *c* oxidase was shown by electron diffraction studies at 6 Å resolution (*57*) and preliminary X-ray diffraction studies at 3.5 Å resolution (*58*). Accordingly, the identification and the characterizations of the substrate oxidation site in quinol oxidases would allow us to understand the facile two-electron oxidation of quinols and a gating mechanism of electron flux allowing the one-electron transfer from quinols to the metal centers in subunit I.

As demonstrated for the cytochrome bc_1 complex (see refs *2* and *59* for reviews), mutational and biochemical studies

[2] T. Mogi, K. Inoue, M. Sato-Watanabe, K. Saiki, and Y. Anraku. Unpublished results.

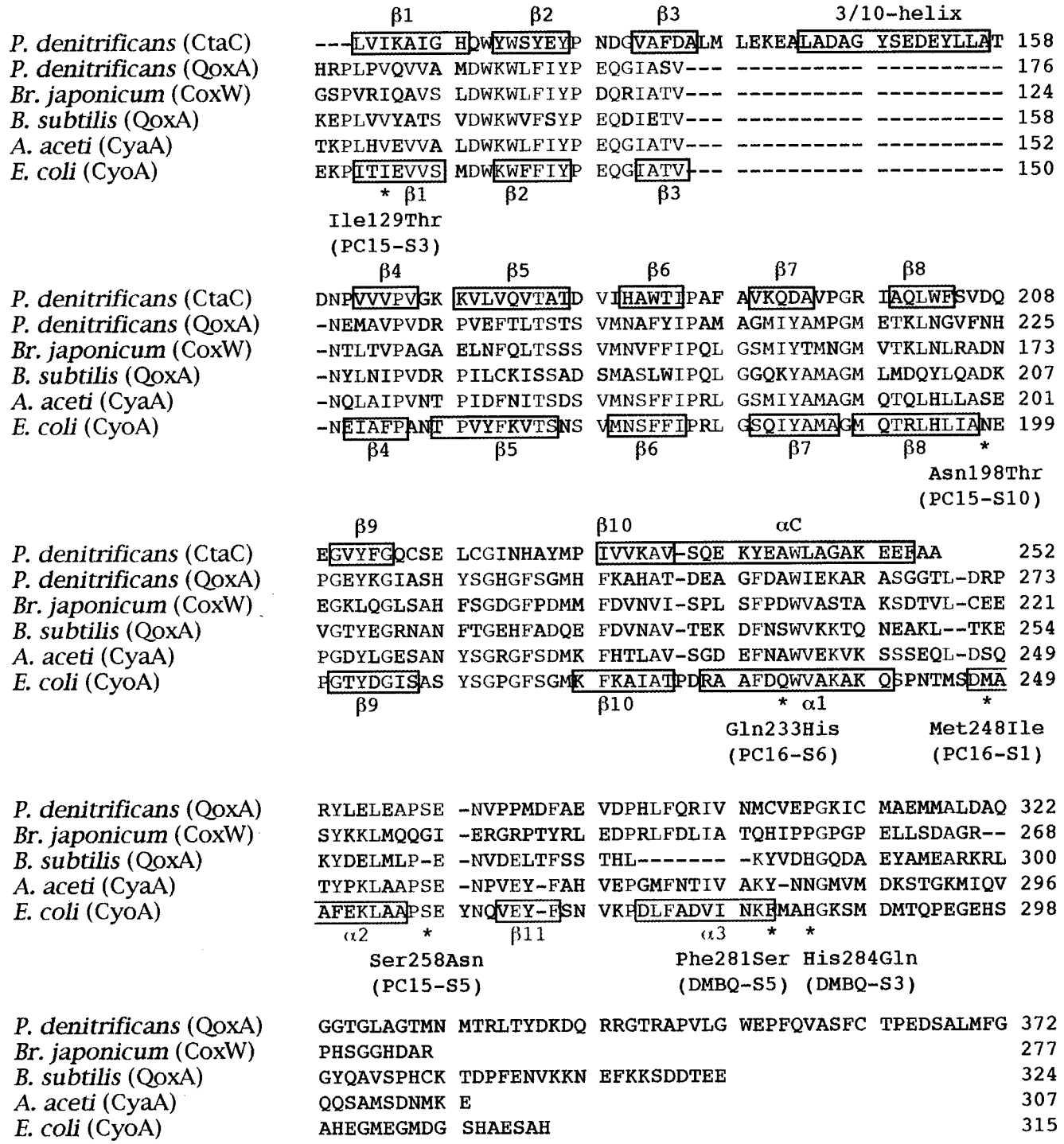

FIGURE 4: Locations of quinone analogue-resistant mutations in the C-terminal hydrophilic region of subunit II. Amino acid sequences of the C-terminal hydrophilic domains aligned are cytochrome *c* oxidase from *P. denitrificans* [the mature CtaC of cytochrome aa_3 (*5*)] and quinol oxidases from *P. denitrificans* [QoxA of cytochrome ba_3 (*34*)], *Br. japonicum* [CoxW of cytochrome bb_3 (*36*)],[3] *B. subtilis* [QoxA of cytochrome aa_3-600 (*37*)], *A. aceti* [CyaA of cytochrome ba_3 (*35*)], and *E. coli* [CyoA of cytochrome *bo* (*33*)]. The residue X at position 238 of CoxW (*36*) was Gln.[3] The Cu_A ligands, His^{181}, Cys^{216}, Cys^{220}, His^{224}, Met^{227}, and Glu^{218} (*29, 32*) are shown in blue. Conserved residues in quinol oxidases are highlighted in red. Secondary structure elements of the mature CtaC (*32*) and the soluble CyoA domain (Pro^{125}-Ala^{283}; ref *31*) are labeled. β-Strands for cupredoxin fold are indicated in blue, and the quinol oxidase-specific Qox domain in red. The quinone analogue-resistant mutations are shown below the CyoA sequence.

using quinone-related inhibitors are useful for identification of the quinone redox sites and elucidation of the reaction mechanism. However, until recently, only a few potent competitive inhibitors are known for the Q_1H_2 oxidation by cytochrome *bo* (*51, 52*). To probe the structural features of the quinol oxidation (Q_L) site of cytochrome *bo*, we have carried out structure−function studies using a wide variety of benzoquinones, substituted phenols (*14, 18*), and Q_2 derivatives (*45*) and identified MBQ, DMBQ, PC15, PC16, and PC31 as the novel Q_L site inhibitors (*14*). We found also that transposition or replacement of one of the methyl

[3] P. H. Tsatsos, K. Raynolds, E. F. Nickels, D.-Y. He, C−A. Yu, and R. B. Gennis. Unpublished results.

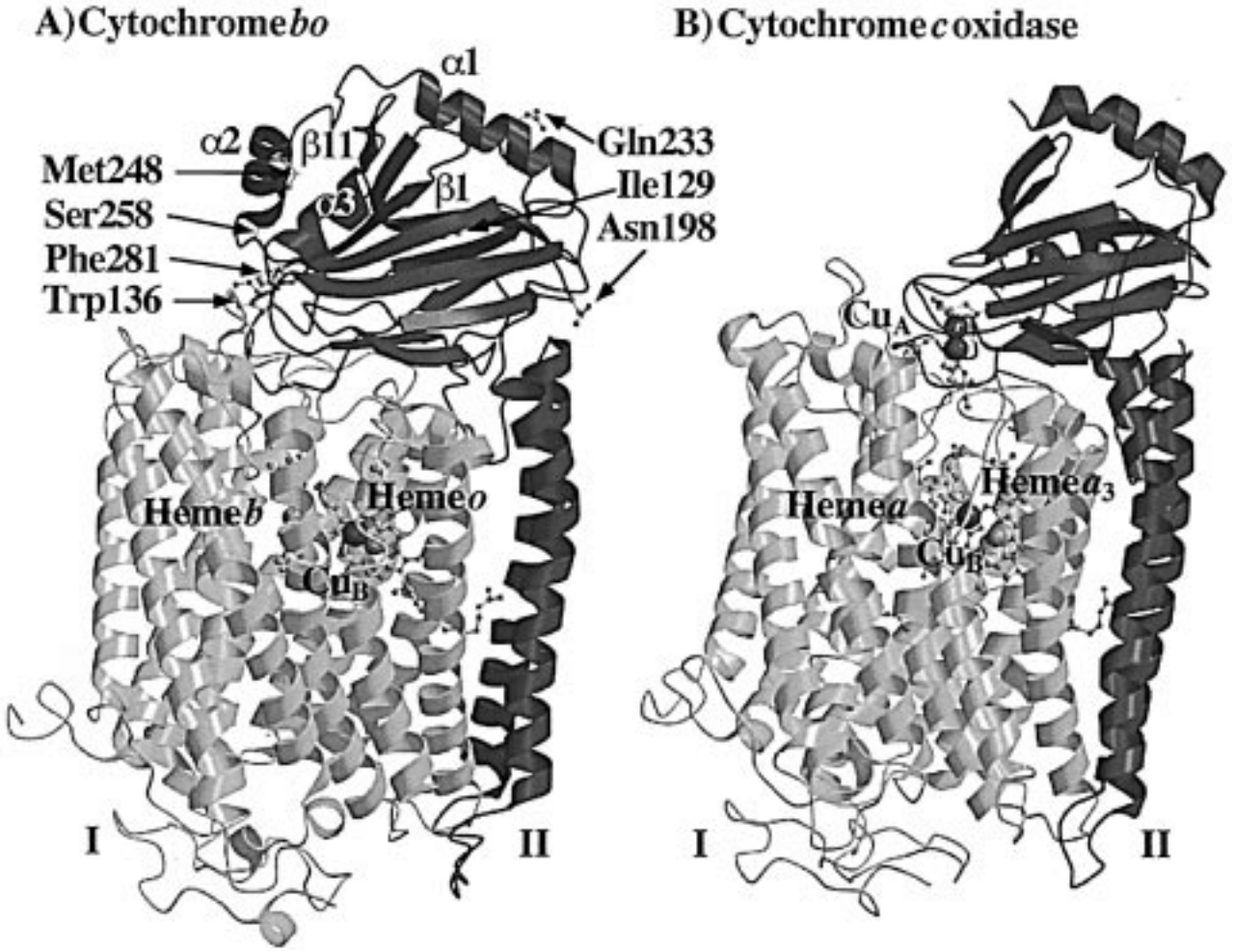

FIGURE 5: Three-dimensional structures for two-subunit preparations of cytochrome *bo* and bacterial cytochrome *c* oxidase. Side chains of the quinone analogue-resistant mutations in CyoA and the Cu_A ligands in CtaC (side chains of His^{181}, Cys^{216}, $Cys^{220}$$His^{224}$ and Met^{227}, the main chain carbonyl of Glu^{218}) are highlighted. A structure model for cytochrome *bo* was constructed based upon the coordinates of four-subunit preparation of aa_3-type cytochrome *c* oxidase from *P. denitrificans* (*29*) and those of the soluble CyoA domain (*31*) as reported previously (*1, 43*). Transmembrane helices 0, XIII, and XIV of subunit I are not included in the model since they are absent in the counterpart of the *Paracoccus* oxidase (*5*). His^{284} of subunit II was omitted from the model, because this residue is just outside the crystal structure of the soluble CyoA domain (*31*). The coordinates for two-subunit preparation of aa_3-type cytochrome *c* oxidase were taken from Ostermeier et al. (*32*).

groups of DMBQ resulted in marked reduction of the inhibitory activity (*14*), showing that the Q_L site can specifically recognize one C═O group with two methyl groups as the ortho substituents. In substituted phenols, chlorine is the most effective as both ortho substituents, and the electron-withdrawing ability of the para substituent determines the inhibitory activity, probably due to stabilization of an anionic form (*14*). The methoxy group in the 2-position of ubiquinone ring is recognized more strictly than that in the 3-position by the Q_L site (*45*). On the basis of our structure−function studies, we postulated that the Q_L site asymmetrically recognizes exogenous ligands and that this property could account for the sequential and directional one-electron transfer from ubiquinols at the Q_L site to heme *b*. The high-affinity ubiquinone binding site Q_H, discovered by Sato-Watanabe et al. (*15*), mediates electron transfer from the Q_L site to heme *b* (*18, 20*).

Among seven Q_L site inhibitors examined in the present study, only DMBQ, PC15, and PC16 were able to inhibit succinate respiration of the intact cells and showed bacteriostatic effects on the aerobic growth (Table 1). Spontaneous mutants resistant to these ubiquinone analogues increased the I_{50} values of the aerobic growth on succinate and the K_i values of the Q_1H_2 oxidation for the selecting compounds (Table 1). Large differences between the I_{50} and K_i values are attributable to permeability in the outer membrane that is mostly covered with hydrophilic lipopolysaccharide or to multidrug-efflux pumps present in the cytoplasmic membrane (*60*). Cross-resistance in the PC15- and PC16-resistant mutants is consistent with our previous proposal that the binding site for substituted phenols recognized the overlapping substituting groups on the phenol ring (*14*). Several mutants showed cross-resistance against DMBQ and substituted phenols, suggesting that their binding sites are partially overlapped in the Q_L site. Since all the quinone analogue-resistant mutants can grow aerobically with endogenous Q_8H_2 in the membrane, none of the mutations largely affected the K_m values for the Q_1H_2 and Q_2H_2 derivatives (Tables 1 and 2).

Genetic complementation test showed that the mutations are localized in either the 0.47 kb *Kpn*I−*Nhe*I fragment (Pro^{96}-Lys^{253} of subunit II) or the 0.32 kb *Nhe*I−*Sal*I (Leu^{254}-His^{315} of subunit II and Met^{1}-Ser^{51} of subunit I). Deletion studies on subunit I[2] and gene fusion experiments (*53*)

favored the presence of the mutations in Pro[96]-His[315] of subunit II. Sequencing analysis revealed that the mutations are localized near both ends of the cupredoxin fold (Figure 5). Met248Ile (PC16−S1), Ser258Asn (PC15−S5), Phe281Ser (DMBQ−S5), and His284Pro (DMBQ−S3) are present within or near the Qox domain and proximal to the lost Cu_A site (*25, 31*) in subunit II and heme *b* in subunit I. In our two-subunit model for cytochrome *bo* (Figure 5), Met[248] in α_2 interacts with Leu[273] and Asp[276] in α_3, Ser[258] in α_2/β_{11} loop with Lys[137] in β_2, and Phe[281] in α_3 with Asn[168] in β_5/β_6 loop and Asn[268] in β_{11}/α_3 loop. His[284], though not in the model, is present next to the C-terminus of α_3 (Figure 4). Substitutions of Met[248], Ser[258], Phe[281], and His[284] could perturb the Qox domain or the Cu_A end of the cupredoxin fold. In contrast, Ile129Thr (PC15−S3), Asn198Thr (PC15−S10), and Gln233His (PC16−S6) are rather scattered around another end of the cupredoxin fold and closer to transmembrane helices of subunit II (Figures 4 and 5). Ile[129] in β_1 interacts with Tyr[142] in β_2/β_3 loop and Val[161] and Phe[163] in β_5, and Asn[198] in β_8/β_9 loop with Asn[158] in β_4/β_5 loop. Thus, the mutations at Ile[129] and Asn[198] would affect the Cu_A end structure through perturbation of the cupredoxin fold. Substitution of His[284] by Pro could alter the secondary structure of α_1, thereby perturbing the cupredoxin fold through interactions of α_1 with the cupredoxin fold.

Furthermore, recent cross-linking studies with the azido-ubiquinone showed the proximity of the ubiquinone ring to Val[165]-Arg[178] (β_5/β_6 loop region) and possibly Leu[254]-Met[270] (α_2-β_{11}-α_3 region) of subunit II.[4] These fragments are present in the Cu_A end of the cupredoxin fold and the Qox domain, respectively (Figure 4), and are close to our Met248Ile, Ser258Asn, Phe281Ser, and His284Pro mutations. In addition, site-directed mutagenesis studies revealed that the substitution of the conserved Trp[136] in β_1/β_2 loop (i.e., the Cu_A end) with Ala largely decreased the affinity for substrate.[5] These findings indicate the importance of the Cu_A end of the cupredoxin fold and the Qox domain in substrate binding.

In cytochrome *c* oxidase from *P. denitrificans*, Trp[121] (Trp[136] in cytochrome *bo*) exists in a surface-exposed hydrophobic patch and is within 3.2 Å of the Cu_A ligand Met[227] (Met[218]) in β_{10} and in hydrogen-bond distance to the Cu_A ligand His[181] (Asn[172]) in β_6 (*29, 32*). The proposal that Trp[121] mediates electron transfer from cytochrome *c* to Cu_A (*29, 32*) was recently verified by site-directed mutagenesis studies (*61*). Alternatively, Trp[136] of cytochrome *bo* may serve as an electron-transfer pathway to subunit I or a part of binding site for the ubiquinone ring. In cytochrome *c* oxidases, a hydrogen bond system including His[224] (in *P. denitrificans*) of subunit II, a peptide bond between Arg[473] and Arg[474] in loop XI-XII of subunit I, and a propionate of heme *a* has been proposed for electron transfer from Cu_A to heme *a* (*29, 30*). Substitution of His[224] by Phe in quinol oxidases (Figure 4) indicates the presence of an alternative pathway for electron transfer from the Q_L site to heme *b*.

In conclusion, enzymatic properties of the quinone analogue-resistant mutant oxidases, locations of these mutations (this study), cross-linking studies with the azido-ubiquinone (*13*),[4] and site-directed mutagenesis studies on subunit II[5] favor the assignment that the Q_L site is provided by the Qox domain and/or the Cu_A end of the cupredoxin fold in subunit II. It was postulated that quinol oxidases except cytochrome *bd* are derived from cytochrome *c* oxidase through duplication of the oxidase operon in Gram-positive bacteria and have spreaded to Proteobacteria by lateral gene transfer (*1, 7*). This study suggests that the transformation of cytochrome *c* oxidase to quinol oxidase can be achieved by addition of the Qox domain to the C-terminus of subunit II and/or minor modifications of the Cu_A end of the cupredoxin fold. Accordingly, quinol oxidases and cytochrome *c* oxidases must share pathways for intramolecular electron transfer and the molecular machinery for dioxygen reduction. Detailed structural and functional studies on the Q_L site and random mutagenesis studies with the Q_H site-specific quinone analogues (18) will provide us a clue for understanding the unique catalytic and electron-transfer mechanisms in terminal quinol oxidases.

[4] J. Ma, A. Puustinen, M. Wikström, and R. B. Gennis. Unpublished results.

[5] M. A. Surpin, and R. J. Maier. Personal communication.

ACKNOWLEDGMENT

We thank R. B. Gennis (University of Illinois) for *E. coli* strain GO103, personal communication and critical comments, H. Michel (Max-Planck Institute) for the latest coordinates of the two-subunit bacterial cytochrome *c* oxidase, M. A. Surpin (Salk Institute for Biological Studies) and R. J. Maier (Johns Hopkins University) for the revised CoxW sequence, and H. Shimizu and S. Harada (University of Tokyo) for preparation of Figure 5.

REFERENCES

1. Mogi, T., Tsubaki, M., Hori, H., Miyoshi, H., Nakamura, H., and Anraku, Y. (1998) *J. Biochem. Mol. Biol. Biophys. 2*, (in press).
2. Trumpower, B. L., and Gennis, R. B. (1994) *Annu. Rev. Biochem. 63*, 675−716.
3. Hosler, J. P., Ferguson-Miller, S., Calhoun, M. W., Thomas, J. W., Hill, J., Lemieux, L., Ma, J., Georgiou, C., Fetter, J., Shapleigh, J., Tecklenburg, M. M. J., Babcock, G. T., and Gennis, R. B. (1993) *J. Bioenerg. Biomembr. 25*, 121−136.
4. Mogi, T., Nakamura, H., and Anraku, Y. (1994) *J. Biochem. (Tokyo) 116*, 471−477.
5. Saraste, M. (1990) *Q. Rev. Biophys. 23*, 331−366.
6. Saraste, M., Holm, L., Lemieux, L., Lübben, M., and van der Oost, J. (1991) *Biochem. Soc. Trans. 19*, 608−612.
7. Castresana, J., Lübben, M., Saraste, M., and Higgins, D. G. (1994) *EMBO J. 13*, 2516−2525.
8. Puustinen, A., Finel, M., Haltia, T., Gennis, R. B., and Wikström, M. (1991) *Biochemistry 30*, 3936−3942.
9. Saiki, K., Nakamura, H., Mogi, T., and Anraku, Y. (1996) *J. Biol. Chem. 271*, 15336−15340.
10. Saiki, K, Mogi, T., Tsubaki, M., Hori, H., and Anraku, Y. (1997) *J. Biol. Chem. 272*, 14721−14726.
11. Nakamura, H., Saiki, K., Mogi, T., and Anraku, Y. (1997) *J. Biochem. (Tokyo) 122*, 415−421.
12. Kita, K., Konishi, K., and Anraku, Y. (1984) *J. Biol. Chem. 259*, 3368−3374.
13. Welter, R., Gu, L.-Q., Yu, L., Yu, C.-A., Rumbley, J., and Gennis, R. B. (1994) *J. Biol. Chem. 269*, 28834−28838.
14. Sato-Watanabe, M., Mogi, T., Miyoshi, H., Iwamura, H., Matsushita, K., Adachi, O., and Anraku, Y. (1994) *J. Biol. Chem. 269*, 28899−28907.
15. Sato-Watanabe, M., Mogi, T., Ogura, T., Kitagawa, T., Miyoshi, H., Iwamura, H., and Anraku, Y. (1994) *J. Biol. Chem. 269*, 28908−28912.

16. Puustinen, A., Verkhovsky, M., Morgan, J. E., Belevich, N. P., and Wikström, M. (1996) *Proc. Natl. Acad. Sci. U.S.A. 93*, 1545−1548.
17. Svensson-Ek, M., and Brzezinski, P. (1997) *Biochemistry 36*, 5425−5431.
18. Sato-Watanabe, M., Mogi, T., Miyoshi, H., and Anraku, Y. (1998) *Biochemistry 37*, 5356−5361.
19. Sato-Watanabe, M., Mogi, T., Miyoshi, H., and Anraku, Y. (1998) in *Oxygen Homeostasis and Its Dynamics* (Ishimura, Y., Shimada, H., and Suematsu, M., Eds.) pp 24−32, Springer-Verlag, Tokyo.
20. Sato-Watanabe, M., Itoh, S., Mogi, T., Matsuura, K., Miyoshi, H., and Anraku, Y. (1995) *FEBS Lett. 374*, 265−269.
21. Ingledew, W. J., Ohnishi, T., and Salerno, J. C. (1995) *Eur. J. Biochem. 227*, 903−908.
22. Osborne, J. P., Musser, S. M., Schultz, B. E., Edmondson, D. E., Chan, S. I., and Gennis, R. B. (1998) in *Oxygen Homeostasis and Its Dynamics* (Ishimura, Y., Shimada, H., and Suematsu, M., Eds.) pp 33−39, Springer-Verlag, Tokyo.
23. Kelly, M., Lappalainen, P., Talbo, G., Haltia, T., van der Oost, J., and Saraste, M. (1993) *J. Biol. Chem. 268*, 16781−16787.
24. Farrar, J. A., Lappalainen, P., Zumft, W. G., Saraste, M., and Thomson, A. J. (1995) *Eur. J. Biochem. 232*, 294−303.
25. van der Oost, J., Lappalainen, P., Lemieux, L., Rumbley, J., Gennis, R. B., Aasa, R., Pascher, T., Malmström, B. and Saraste, M. (1992) *EMBO. J. 11*, 3209−3217.
26. Lappalainen, P., Aasa, R., Malmström, B., and Saraste, M. (1993) *J. Biol. Chem. 268*, 26416−26421.
27. Wittung, P., Källebring, B., and Malmström, B. (1994) *FEBS Lett. 349*, 286−288.
28. Beinert, H. (1997) *Eur. J. Biochem. 245*, 521−532.
29. Iwata, S., Ostermeier, C., Ludwig, B., and Michel, H. (1995) *Nature 376*, 660−669.
30. Tsukihara, T., Aoyama, H., Yamashita, E., Tomizaki, T., Yamaguchi, H., Shinzawa Itoh, K., Nakashima, R., Yaono, R., and Yoshikawa, S. (1995) *Science 269*, 1069−1074.
31. Wilmanns, M., Lappalainen, P., Kelly, M., Sauer-Eriksson, E., and Saraste, M. (1995) *Proc. Natl. Acad. Sci. U.S.A. 92*, 11955−11959.
32. Ostermeier, C., Harrenga, A., Ermler, U., and Michel, H. (1997) *Proc. Natl. Acad. Sci. U.S.A. 94*, 10547−10553.
33. Chepuri, V., Lemieux, L., Au, D. C.-T., and Gennis, R. B. (1990) *J. Biol. Chem. 265*, 11185−11192.
34. Richter, O. H., Tao, J.-S., Turba, A., and Ludwig, B. (1994) *J. Biol. Chem. 269*, 23079−23086.
35. Fukaya, M., Tayama, K., Tamaki, T., Ebisuya, H., Okumura, H., Kawamura, Y., Horinouchi, S., and Beppu, T. (1994) *J. Bacteriol. 175*, 4307−4314.
36. Surpin, M. A., Lübben, M., and Maier, R. J. (1996) *Gene 183*, 201−206.
37. Santana, M., Kunst, F., Hullo, M. F., Rapoport, G., Danchin, A., and Glaser, P. (1992) *J. Biol. Chem. 267*, 10225−10231.
38. Egami, F. (1977) *Origins Life 8*, 169−171.
39. Ishimoto, M., and Egami, F. (1957) *Proceedings of the International Symposium on the Origin of Life on the Earth*, pp 322, Academy of Science of the USSR, Moscow.
40. Saraste, M., and Castresana, J. (1994) *FEBS Lett. 341*, 1−4.
41. Minagawa, J., Mogi, T., Gennis, R. B., and Anraku, Y. (1992) *J. Biol. Chem. 267*, 2096−2104.
42. Mogi, T., Hirano, T., Nakamura, H., Anraku, Y., and Orii, Y. (1995) *FEBS Lett. 370*, 259−263.
43. Mogi, T., Minagawa, J., Hirano, T., Sato-Watanabe, M., Tsubaki, M., Uno, T., Hori, H., Nakamura, H., Nishimura, Y., and Anraku, Y. (1998) *Biochemistry 37*, 1632−1639.
44. Tsubaki, M., Mogi, T., Anraku, Y., and Hori, H. (1993) *Biochemistry 32*, 6065−6072.
45. Sakamoto, K., Miyoshi, H., Takegami, K., Mogi, T., Anraku, Y., and Iwamura, H. (1996) *J. Biol. Chem. 271*, 29897−29902.
46. Crane, F. L., and Barr, R. (1971) *Methods Enzymol. 18C*, 137−165.
47. Davis, B. D., and Mingioloi, E. S. (1959) *J. Bacteriol. 60*, 17−28.
48. Minagawa, J., Nakamura, H., Yamato, I., Mogi, T., and Anraku, Y. (1990) *J. Biol. Chem. 265*, 11198−11203.
49. Miyoshi, H., Saitoh, I., and Iwamura, H. (1993) *Biochim. Biophys. Acta 1143*, 23−28.
50. Tokutake, N., Miyoshi, H., and Fujita, T (1991) *Biochim. Biophys. Acta 1057*, 377- 383.
51. Kita, K., Kasahara, M., and Anraku, Y. (1982) *J. Biol. Chem. 257*, 7933−7935.
52. Matsushita, K., Patel, L., and Kaback, H. R. (1984) *Biochemistry 23*, 4703−4714.
53. Ma, J., Lemieux, L., and Gennis, R. B. (1993) *Biochemistry 32*, 7692−7697.
54. Tsukihara, T., Aoyama, H., Yamashita, E., Tomizaki, T., Yamaguchi, H., Shinzawa-Itoh, K., Nakashima, R., Yaono, R., and Yoshikawa, S. (1996) *Science 272*, 1136−1144.
55. Farrar, J. A., Lappalainen, P., Zumft, W. G., Saraste, M., and Thomson, A. J. (1995) *Eur. J. Biochem. 232*, 294−303.
56. Speno, H., Taheri, M. R., Sieburth, D., and Martin, C. T. (1995) *J. Biol. Chem. 270*, 25363−25369.
57. Gholke, U., Warne, A., and Saraste, M. (1997) *EMBO. J. 16*, 1181−1188.
58. Abramson, J., and Iwata, S. (1998) *EBEC Short Rep. 10*, 81.
59. Brasseur, G., Saribas, A. S., and Daldal, F. (1996) *Biochim. Biophys. Acta 1275*, 61−69.
60. Miller, P. F., and Sulavik, M. C. (1996) *Mol. Microbiol. 21*, 441−448.
61. Witt, H., Malatesta, F., Nicoletti, F., Brunori, M., and Ludwig, B. (1998) *J. Biol. Chem. 273*, 5132−5136.

BI981184L